

# The Tharsis Montes, Mars: Comparison of Volcanic and Modified Landforms

James R. Zimbelman

Center for Earth and Planetary Studies, National Air and Space Museum,  
Smithsonian Institution, Washington DC 20560

Kenneth S. Edgett

Department of Geology, Arizona State University, Tempe AZ 85287-1404

---

The three Tharsis Montes shield volcanos, Arsia Mons, Pavonis Mons, and Ascræus Mons, have broad similarities that have been recognized since the Mariner 9 reconnaissance in 1972. Upon closer examination the volcanos are seen to have significant differences that are due to individual volcanic histories. All three volcanos exhibit the following characteristics: gentle ( $<5^\circ$ ) flank slopes, entrants in the northwestern and southeastern flanks that were the source for lavas extending away from each shield, summit caldera(s), and enigmatic lobe-shaped features extending over the plains to the west of each volcano. The three volcanos display different degrees of circumferential graben and trough development in the summit regions, complexity of preserved caldera collapse events, secondary summit-region volcanic construction, and erosion on the lower western flanks due to mass wasting and the processes that formed the large lobe-shaped features. All three lobe-shaped features start at elevations of 10 to 11 km and terminate at 6 km. The complex morphology of the lobe deposits appear to involve some form of catastrophic mass movement followed by effusive and perhaps pyroclastic volcanism.

## INTRODUCTION

The Tharsis Montes consist of three large shield volcanos named (from south to north) Arsia Mons, Pavonis Mons, and Ascræus Mons (Fig. 1). They are located along the crest of the Tharsis rise, aligned along a  $N40^\circ E$  trend. Each volcano is 350 to 400 km in diameter with their summits spaced about 750 km apart. From base to summit, the Tharsis Montes each stand 10 to 15 km high, with flank slopes of  $<5^\circ$  (USGS, 1989). The bases of the volcanos are located 8 to 10 km above the martian datum because of their location upon the Tharsis rise, placing them at elevations higher than most of the martian surface. An even larger shield volcano, Olympus Mons, is located 1700 km west of Ascræus Mons.

The general morphology and geology of the Tharsis shield volcanos were discussed in Mariner 9 and Viking primary mission reports (Carr, 1973; Carr et al., 1977), and each has been portrayed as a single volcanic unit in geologic maps of Mars (Scott and Carr, 1978; Scott and Tanaka, 1986). The general geologic history of the Tharsis Montes region was summarized in the paleostratigraphic reconstruction by Scott and Tanaka (1981). The Tharsis Montes shields are interpreted to result from lavas erupted from vents along the  $N40^\circ E$ -trending axis of alignment along the crest of the Tharsis rise, a portion of the martian crust more than 6000 km across that rises up to 10 km above the surrounding terrain (Carr, 1974). Hypotheses for the origin of the Tharsis rise remain an area of ongoing investigation (see Zimbelman et al., 1991), but all alternatives include the release of large quantities of volcanic materials. Eruptions began in the Tharsis region during the Hesperian epoch (Scott and Tanaka, 1986), although the earliest phases of volcanism are mostly buried beneath

subsequent materials (Scott and Tanaka, 1981). All the materials on and around the Tharsis Montes are mapped as Upper Hesperian to Upper Amazonian in age (Scott and Tanaka, 1986). The surrounding plains are made up of lava flows that bury the lower flanks of the shields to depths up to 4 km (Whitford-Stark, 1982).

Crumpler and Aubele (1978) proposed that the Tharsis Montes, while approximately similar in age, show different degrees of structural evolution: Arsia Mons is the most evolved while Ascræus Mons shows the least development. Crater counts are particularly difficult to interpret on volcanic constructs, but several studies suggest that there is also a temporal variation, with Arsia Mons being the oldest of the three volcanos and Ascræus Mons the youngest (Blasius, 1976; Plescia and Saunders, 1979; Neukum and Hiller, 1981). These apparent trends in structural and temporal characteristics probably reflect the timing of the cessation of large volcanic eruptions at each shield.

The three Tharsis Montes exhibit gross similarities, many of which have been noted previously (McCauley et al., 1972; Carr, 1973; Carr et al., 1977; Crumpler and Aubele, 1978). For example, the three volcanos each have similar dimensions, "embayments" (terminology of Carr, 1973) on the northeast and southwest flanks along the  $N40^\circ E$  trend, and a large "lobe-shaped deposit" (terminology of Carr et al., 1977) to its west. Crumpler and Aubele (1978) noted, however, that there are differing degrees of caldera development, with Arsia Mons having a single large caldera, Pavonis Mons both a large and small caldera, and Ascræus Mons a complex of six to eight nested calderas. Differences in caldera morphology are interpreted to indicate differences in the size and depth of magma chambers within Arsia and Ascræus Montes (Mouginis-Mark, 1981).

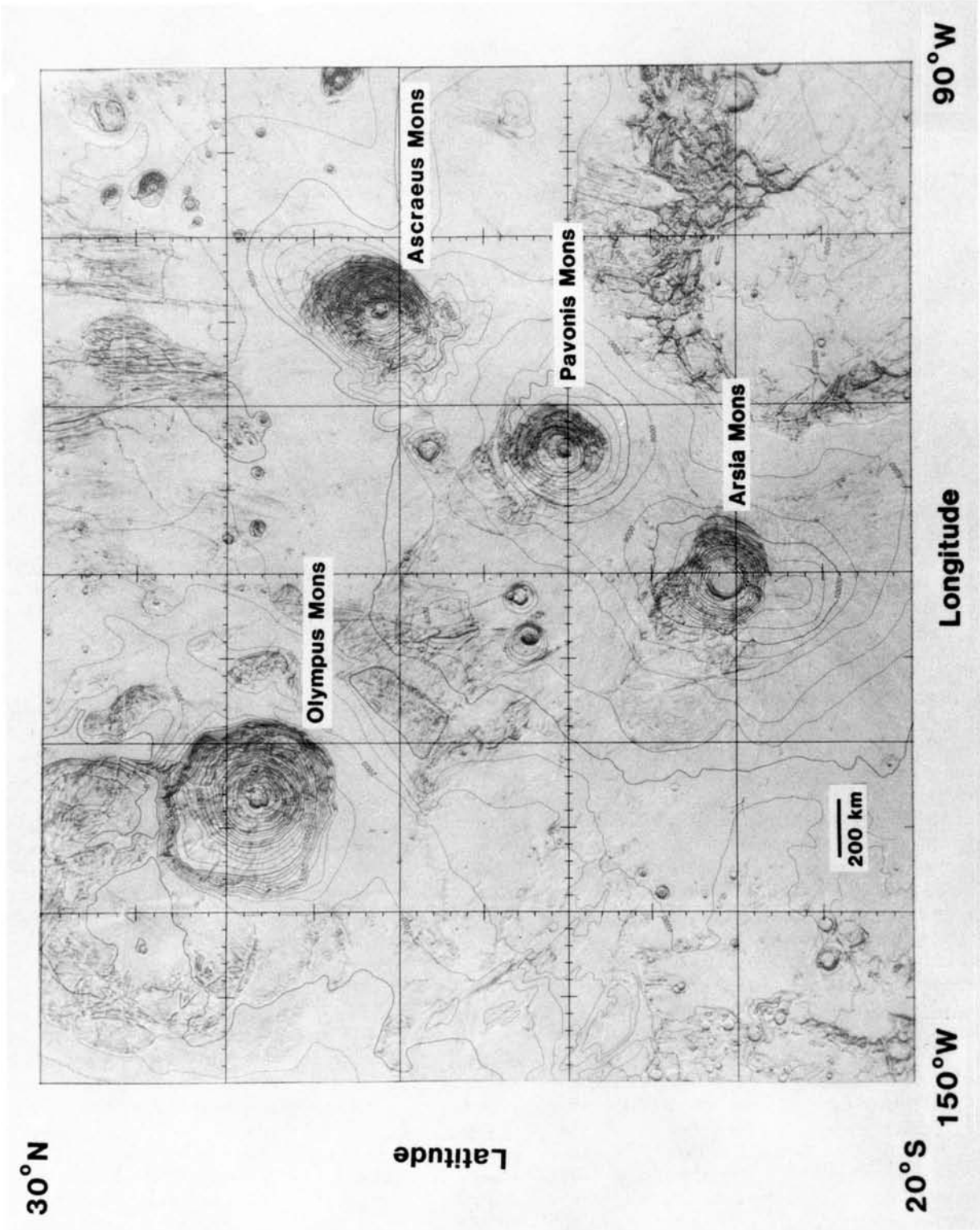


Fig. 1. Regional setting of the Tharsis Montes on Mars. Shaded relief rendition and 1-km topographic contours are from USGS (1989), with names of selected features added for reference. The area shown corresponds to  $10^7$  km<sup>2</sup>, or about 1/14 of the surface area of Mars.

## PURPOSE

This paper presents descriptions and comparisons of landforms on and around the three Tharsis Montes volcanos based on the complete set of Mariner 9 and Viking images. The purpose here is to highlight new observations that provide insight into the differences and similarities between these volcanos in terms of the styles of volcanism present and the modification of volcanic landforms by erosional and tectonic processes. Because only the latest volcanic surfaces can be examined from orbital images, this paper concentrates on a synthesis of the latter stages of volcanic activity rather than the full history represented by the immense volcanic constructs. Detailed modeling of geomorphic processes is beyond the scope of the present paper.

## METHODS AND CONVENTIONS

### Data

This study makes use of the best available images of the Tharsis Montes obtained from both the Mariner 9 and Viking missions. The Viking images range in resolution from 90 to 150 m/pixel over most of the region, with isolated coverage of high-resolution images (22 m/pixel for Ascræus Mons and 40 m/pixel for Arsia Mons). Mariner 9 obtained nine images of Pavonis Mons with a resolution down to 45 m/pixel, which exceeds the 75 m/pixel resolution of the best Viking images.

### Crater Counts

The areal density of impact craters is commonly a useful tool for establishing stratigraphic relationships between planetary surfaces. However, it is usually difficult to distinguish exogenic (impact) from endogenic (volcanic or collapse) craters on volcanic landforms (Greeley and Gault, 1971, 1979; Hartmann, 1973; Blasius, 1976). Blasius (1976) distinguished endogenic craters using the following characteristics: (1) elongate shape, (2) crater chains parallel to structural trends, (3) craters lacking positive relief rims, and (4) craters lacking visible ejecta deposits. We found that Blasius' criteria were useful on high-resolution images of Ascræus Mons (Zimbelman, 1984) but were difficult to apply to more moderate-resolution images of all three volcanos. For example, no craters on Pavonis Mons have visible ejecta deposits. Because of these difficulties, stratigraphic assessments presented here are derived solely from superposition relationships at unit contacts. The limited crater frequency information precludes quantitative correlation of units that have no spatial connections, as in comparison of similar units on different volcanos.

### Map Unit Designations

A synthesis of our results is presented in the form of simplified terrain unit maps (Fig. 2). Units are defined on the basis of morphologic characteristics and superposition relationships on and around the three volcanos. Most of the units have counterparts on each volcano (e.g., caldera floor unit cf) but the names are used to indicate terrain characteristics rather

than correlative materials. The units have been given a numerical subscript to identify their associated volcano: 1 for Arsia Mons, 2 for Pavonis Mons, and 3 for Ascræus Mons. Shield flank units have been designated with the letters a, b, or c, where sa represents the oldest flank unit and sb and sc indicate younger units. For example, on Arsia Mons the oldest shield flank is designated sa<sub>1</sub>. As with other units, the shield flank units are not necessarily correlative, but in this case they may not even be similar in overall appearance between volcanos.

## OBSERVATIONS AND INTERPRETATIONS

Landforms common to all three Tharsis Montes are summarized here to allow subsequent sections to concentrate on observations relevant to each individual volcano. Common features on and around the volcanos include grabens, elliptical troughs, and sinuous rilles. Grabens are linear troughs with flat floors and simple, inward-facing scarps. Elliptically shaped troughs have rounded terminations and usually follow the trend of nearby grabens. Both grabens and elliptical troughs are typically 2 to 10 km wide. Sinuous rilles are narrow, winding valleys that trend downslope and may have served as conduits for fluid lavas (e.g., Greeley, 1971).

Each of the Tharsis Montes has four main physiographic regions: (1) shield flanks, (2) flank vents, (3) summit, and (4) a lobe-shaped feature. The flanks of each shield have slopes of 3° to 5°, with 30- to 50-km-wide terraces present within 100 km of the summit caldera rim. The term "flank vent" is used here for the entrants termed "embayments" by Carr (1973) and "parasitic calderas" by Crumpler and Aubele (1978), which are present on the northeast and southwest flanks of each volcano, approximately aligned with the N40°E trend. These entrants were the source of lava flows that radiate away from the volcanos. Each volcano has one or more calderas near the topographic summit of the construct. We consider a caldera to be "a large volcanic collapse depression, more or less circular in form, the diameter of which is many times greater than that of any included vent" (Williams and McBirney, 1979, p. 207). Finally, each volcano has a "lobe-shaped feature" west-northwest of the shield, each of which is confined between elevations of 6 and 11 km (USGS, 1989). The following sections describe the distinctive aspects of each of these physiographic regions for the three volcanos.

### Arsia Mons

**Shield flanks.** The shield surface of Arsia Mons (sa<sub>1</sub>) has an asymmetric distribution with respect to the summit caldera (cf<sub>1</sub>), being nearly twice as broad perpendicular to the N40°E trend as parallel to it (Fig. 2a). Grabens on the eastern flank are absent within 100 km of the caldera rim (Fig. 3). The western flank includes several large (up to 10 km wide), shallow grabens concentric to the caldera and present along the entire flank up to the caldera rim. Below 15 km (USGS, 1989), the western shield surface is degraded relative to the upper flanks, with few concentric grabens and an irregular surface (Fig. 4). This degraded western flank (sb<sub>1</sub>) terminates along an irregular scarp at 10 km elevation that forms the upper contact of a smooth unit (sc<sub>1</sub>), interpreted here to be

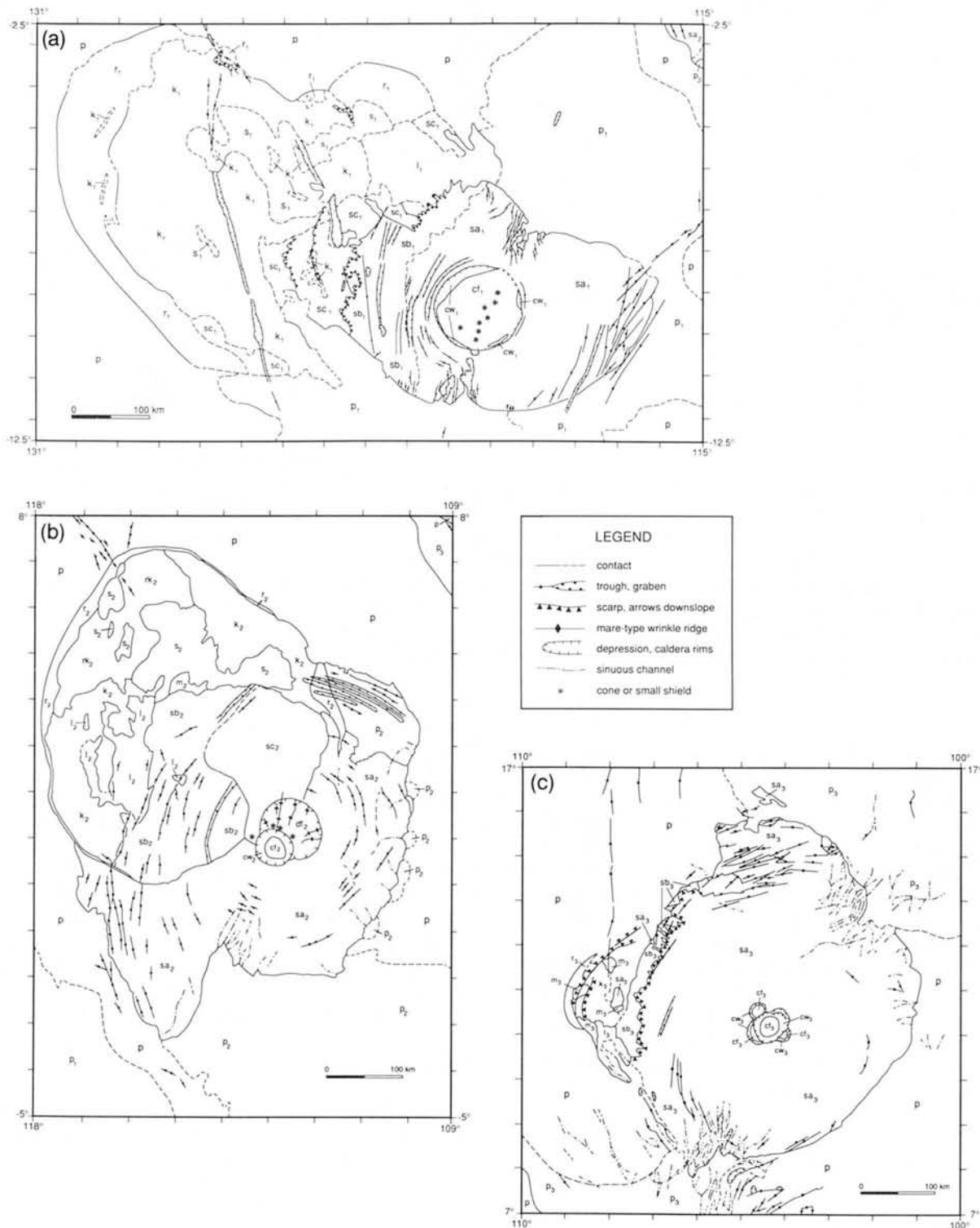


**Fig. 2.** Simplified sketch maps of terrain units on and around the Tharsis Montes. **(a)** Arsia Mons. Units: sa<sub>1</sub> (shield), sb<sub>1</sub> (degraded western flank), sc<sub>1</sub> (smooth lower western flank), cf<sub>1</sub> (caldera floor), cw<sub>1</sub> (caldera wall), p<sub>1</sub> (flank vent flows from Arsia Mons), p (undivided Tharsis plains), r<sub>1</sub> (ridged), k<sub>1</sub> (knobby), l<sub>1</sub> (lobate), s<sub>1</sub> (smooth). **(b)** Pavonis Mons. Units: sa<sub>2</sub> (shield), sb<sub>2</sub> (degraded western flank), sc<sub>2</sub> (resurfaced northern flank), cf<sub>2</sub> (caldera floor), cw<sub>2</sub> (caldera wall), df (depression floor), p<sub>2</sub> (flank vent flows from Pavonis Mons), p (undivided Tharsis plains), r<sub>2</sub> (ridged), k<sub>2</sub> (knobby), rk<sub>2</sub> (ridged-knobby), l<sub>2</sub> (lobate), s<sub>2</sub> (smooth). **(c)** Ascraeus Mons. Units: sa<sub>3</sub> (shield), sb<sub>3</sub> (degraded western flank), cf<sub>3</sub> (caldera floor), cw<sub>3</sub> (caldera wall), p<sub>3</sub> (flows from Ascraeus Mons), p (undivided Tharsis plains), r<sub>3</sub> (ridged), k<sub>3</sub> (knobby), l<sub>3</sub> (lobate), s<sub>3</sub> (smooth).



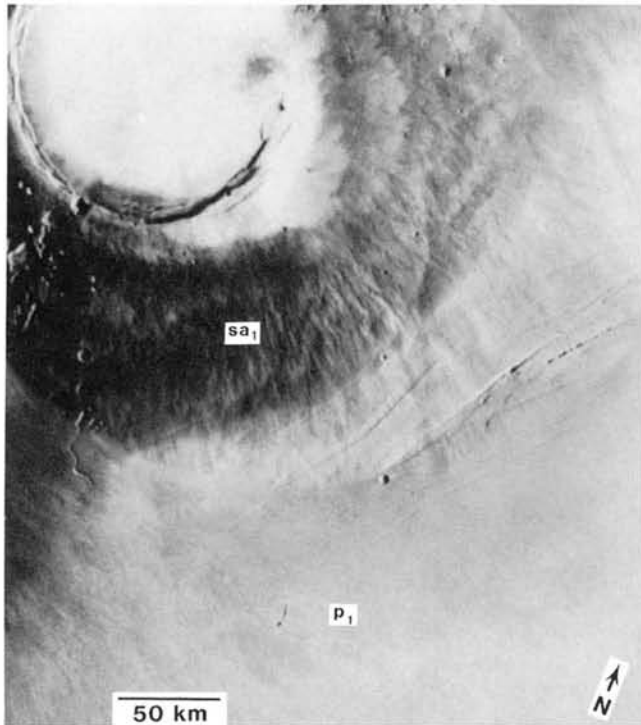


**Fig. 3.** East flank of Arsia Mons. The flows emanating from the southern flank vent on Arsia Mons are superposed on the eastern flank of the volcano. Grabens abundant on the lower eastern flank are not evident within about 100 km of the caldera rim (Viking 641A85, center at 10.1°S, 118.2°W).

a modified portion of the shield since it maintains the same average slope as the flanks above it. The scarp separating units  $sb_1$  and  $sc_1$  has generally <300 m of relief, with many reentrants indicative of localized collapse.

**Summit.** Arsia Mons is surmounted by a circular caldera 100 km in diameter. The rim of the caldera is clearly defined except along the northeastern side (dashed contact, Fig. 2a), where caldera floor ( $cf_1$ ) material may have contacted the upper flanks ( $sa_1$ ). The height of the caldera wall is variable, ranging from several hundred meters above the floor on the southwest to effectively zero on the northeast. Within the northwestern rim of the caldera are materials that were down-dropped during caldera collapse and partially covered by subsequent flows that emanated from vents along the base of the caldera wall (Mouginis-Mark, 1981). The floor of the caldera is smooth except for several very shallow-sloped domes (Fig. 2a), visible only in highly processed versions of low incidence-angle images (Carr *et al.*, 1977). The small domes lack prominent summit pits but they are aligned across the caldera floor parallel to the N40°E trend. The domes have been interpreted to be small shields along a rift zone that crosses the caldera (Carr *et al.*, 1977).

**Flank vents.** The flank vents on the southern and north-northeastern sides of Arsia Mons are formed from linear and sinuous troughs that have coalesced to make prominent scours in the flanks. Depressions that make up the central portions

of the entrants come to within 20 km of the caldera rim on the northern flank and breach the southern caldera rim. Flows emanate from both entrants ( $p_1$ ), burying the eastern flank and embaying the southern margin of the lobe-shaped feature. Contacts between the  $p_1$  plains and surrounding Tharsis plains of unspecified origin ( $p$ ) are gradational and poorly defined in most images; approximate locations of these contacts have been included in Fig. 2a to illustrate the maximum likely extent of plains that are traceable to Arsia Mons.

**Lobe-shaped feature.** West-northwest of Arsia Mons is a lobe-shaped feature that extends along N65°W for 350 km from the base of the volcano. The deposits occur between an elevation of 11 km (on the northern flank) and 6 km at the distal margin. The Arsia Mons lobe includes four distinct terrain types: a ridged unit ( $r_1$ ) along the margin of the lobe, knobby terrain ( $k_1$ ), lobate terrain ( $l_1$ ) composed of interwoven linear segments defined by lobate flow fronts, and a smooth component ( $s_1$ ) superposed on all other terrains (Fig. 2a). The ridged unit is superposed on the surrounding plains (Fig. 5a), but superposition relationships with the knobby and lobate terrains are unclear. The lobate terrain is confined to the northern portion of the Arsia Mons shield (the

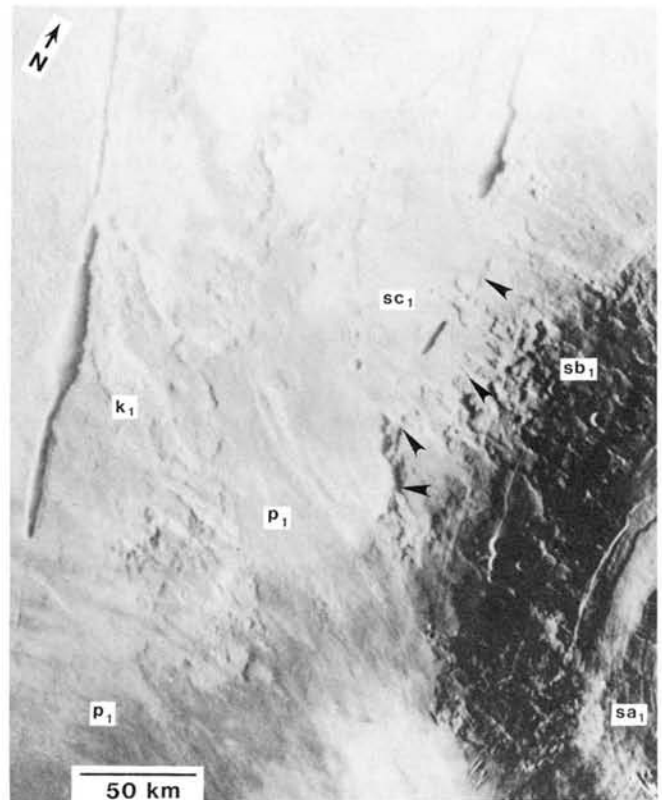


**Fig. 4.** West flank of Arsia Mons. The west flank appears degraded, relative to the east flank (Fig. 3), as evidenced by numerous troughs and grooves scoured into the lower flank. An irregular scarp (arrows) forms the contact between the degraded flank surface and smooth shield materials down slope from the scarp (Viking 641A62, center at 9.1°S, 124.4°W).

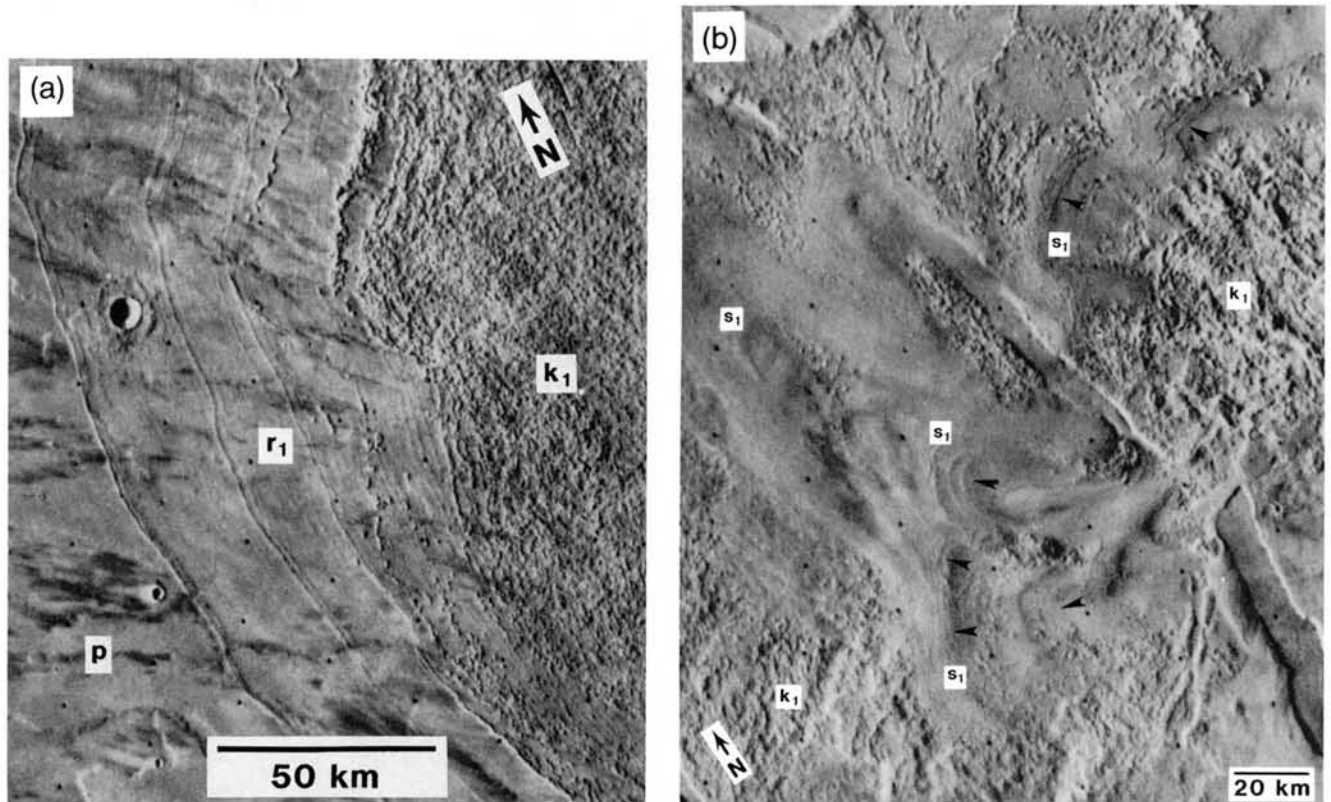


Fig. 5. Portions of lobe-shaped feature northwest of Arsia Mons. (a) Ridged margin of Arsia Mons lobe. Ridges appear superposed on surrounding plains, including a small crater and its ejecta (Viking 42B35, center at 6.1°S, 129.4°W). (b) Smooth unit ( $s_1$ ) superposed on materials within the Arsia Mons lobe. Subtle lineations (arrows) are present at some locations (Viking 42B39, center at 5.9°S, 124.6°W).

only materials present at elevations above 10 km); the unit may represent lava flows that emanated from the basal scarp at this location.

The  $s_1$  unit is superposed on all adjacent terrains, as well as two large grabens that cross the lobe (Fig. 2a). The unit is confined to the interior of the lobe with arcuate lineations visible at some locations (Fig. 5b). The close association with an irregular collapse depression raises the possibility that the smooth unit could be a pyroclastic deposit with the collapse depressions as the source vent(s). An isolated outlier of  $s_1$  material is present on the western portion of the lobe-shaped feature (see Fig. 2a), suggesting that the unit may have once covered much of the lobe surface but has since undergone substantial erosion.

### Pavonis Mons

**Shield flanks.** The Pavonis Mons shield is divided into three terrain units (Fig. 2b). The southern and eastern flanks ( $sa_2$ ) are characterized by a predominance of arcuate grabens (<2 km wide), elliptical troughs, and pits. Sinuous rilles extend downslope to the base of the shield in unit  $sa_2$ , and fanlike deposits made up of individual flows ( $p_2$ ) are found where they meet the adjacent plains (Fig. 6). The western flank ( $sb_2$ )

has several wide (5-10 km) arcuate grabens. Three large troughs near the base of the western flank have large, raised-relief, rough-textured features superposed on them; these are interpreted to be relatively viscous volcanic extrusions (Fig. 7). The northern flank ( $sc_2$ ) has only faint traces of grabens and has few pits, troughs, and rilles (Fig. 8). Subtle linear textures on the northern flank suggest the presence of lava flows that obscure older grabens such that the  $sc_2$  unit postdates the other flanks.

**Summit.** The summit of Pavonis Mons has two calderas: one 45 km in diameter, and the other, offset toward the north, is 85 km in diameter (Fig. 9; McCauley et al., 1972; Carr, 1973). The upper walls of the smaller, simple caldera are fluted, most likely due to mass wasting following caldera collapse (Sharp, 1973a). The larger caldera has six mare-type wrinkle ridges on the floor. One of these ridges extends 12 km onto the shield surface (Fig. 9b). Where wrinkle ridges cross the scarps at the caldera wall, they are vertically offset, indicating that the ridges predate the collapse event. Wood (1979) identified a small circular cone located on a fissure near the western rim of the small caldera, interpreted to be a cinder cone. Four additional elliptical to circular cones have been located within 5 km of the small caldera rim (Fig. 9b). Also, an irregular, rough-textured mound bisected by a fissure ("m")

in Fig. 9c) may be a volcanic extrusion similar to features at the base of the western flank ("v" in Fig. 7). The cones may imply limited strombolian activity occurred during the late-stage summit activity at Pavonis Mons, in contrast to the lack of pyroclastic features at the summits of the other two Tharsis Montes (*Mouginis-Mark*, 1981).

**Flank vents.** The northern flank vent (Fig. 8) has high-standing, fluted walls while the southern flank vent occurs at the convergence of numerous sinuous rilles (Fig. 2b). The relative ages of the flows that emanated from these vents ( $p_2$ ) are unconstrained due to the infrequent occurrence of impact craters on these flows and on the surrounding plains (p). *Scott and Tanaka* (1986) mapped both flank vent units as younger than the surrounding plains, but it now appears that plains flows (p) in the north embay the northern portion of unit  $p_2$ .

**Lobe-shaped feature.** The lobe-shaped feature at Pavonis Mons extends 250 km northwest from the base of the volcano along a N35°W trend (Fig. 2b). No definitive impact craters are recognized on the lobe deposits, although craters as small as 600 m can be resolved on the surrounding plains. Like the Arsia Mons lobe, it is enclosed by a marginal ridge ( $r_2$ ) that in this case extends from the 6.5-km elevation up the flanks of Pavonis Mons to the 11-km level (*USGS*, 1989). The interior of the lobe contains four units identified in the Arsia Mons

lobe: ridged terrain ( $r_2$ ), knobby terrain ( $k_2$ ), lobate flow features ( $l_2$ ), and smooth terrain ( $s_2$ ), plus a transitional "ridged and knobby" unit ( $rk_2$ ). The stratigraphic relationships between the units appear to be similar to those in the Arsia Mons lobe, with the smooth unit superposed on all adjacent lobe terrains. The lobate flow features ( $l_2$ ) appear to originate at troughs associated with small constructional features ("v" in Fig. 7).

#### Ascræus Mons

**Shield flanks.** The Ascræus Mons shield ( $sa_3$ ) is relatively symmetric around the summit calderas, with an additional 100-km extension to the north, where topography directed subsequent lava flows around the flank surface (Fig. 2c). Grabens are absent within about 100 km of the caldera rim, similar to the situation on the eastern flank of Arsia Mons. Terraces on the flanks are uniformly distributed across the shield, similar to the lower flanks of Olympus Mons (*Carr et al.*, 1977) but better developed than the isolated terraces present on the other Tharsis Montes. The terraces have been interpreted to be radial thrust faults due to loading by the shield construct (*Carr et al.*, 1977), but the stress regimes that produced these features must be quite variable among the Tharsis Montes

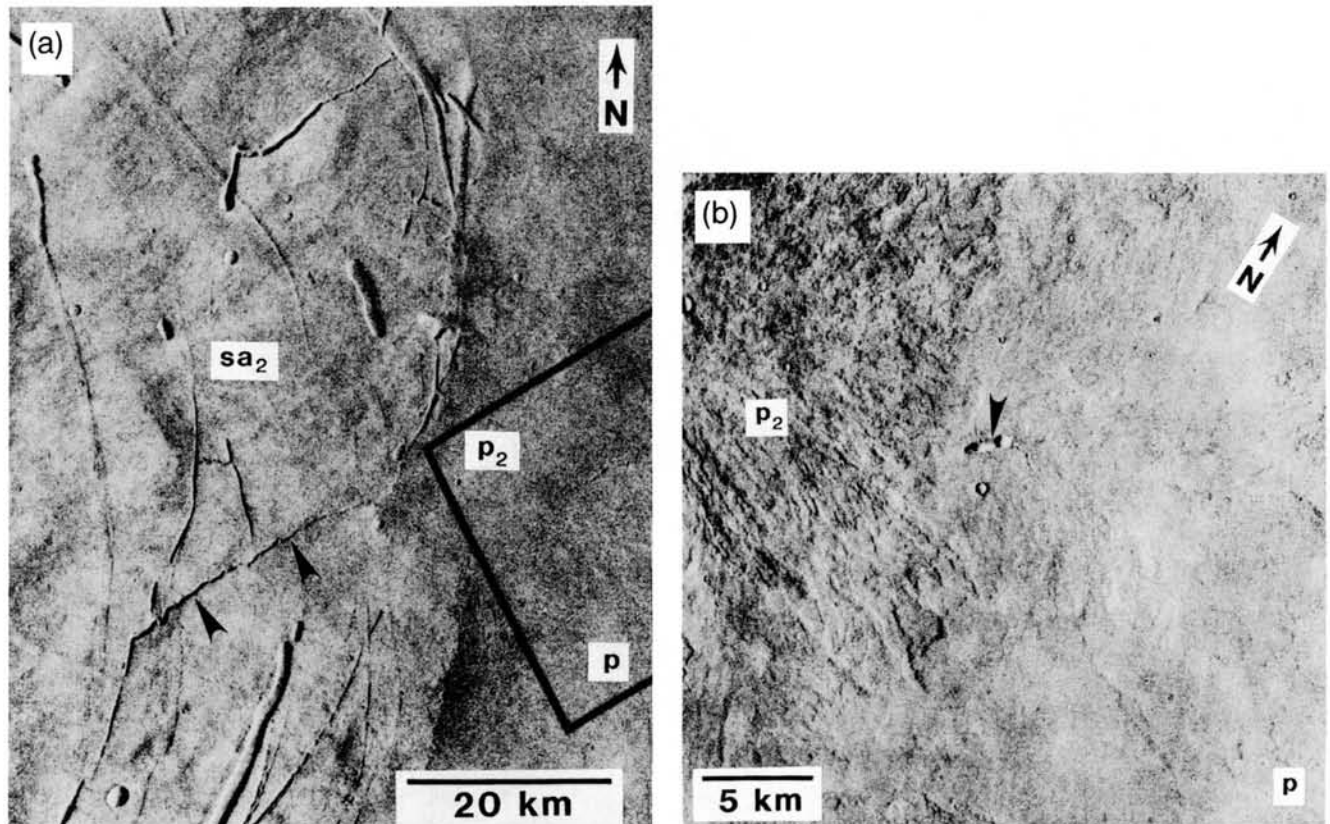


**Fig. 6.** Small embayment on the eastern slope of Pavonis Mons. (a) Regional view showing a small embayment into the shield, originating where a sinuous rille (arrows) on the shield flank contacts the surrounding plains. Box shows location of (b) (Viking 210A38, centered at 1.6°N, 109.7°W). (b) Detailed view of flows at the margin of the small embayment flow unit ( $p_2$ ). In the center of the frame there is a small volcanic vent (arrow) (Viking 388B05, center at 1.0°N, 109.9°W).



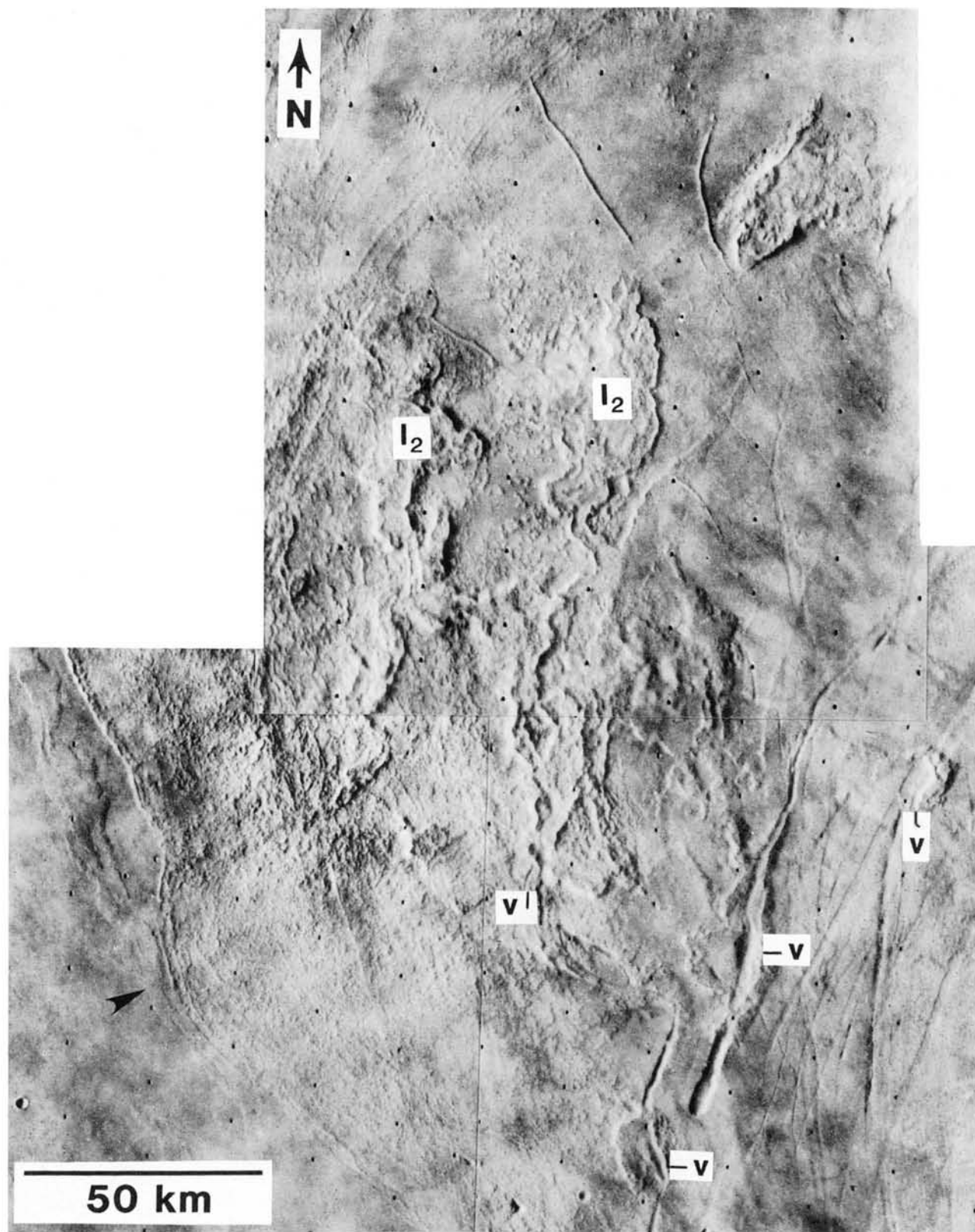


**Fig. 7.** Lobate terrain ( $l_2$ ) within the lobe-shaped feature northwest of Pavonis Mons. These features are interpreted to be volcanic flows that originate either from the troughs along the edge of the shield or from mostly buried troughs in the lobe terrain. Possible volcanic constructs (v) also appear to have originated from the troughs. Arrow indicates a lava flow partly buried by ridged material of the lobe (mosaic of Viking 49B34-6, center at 2.2°N, 116.2°W).



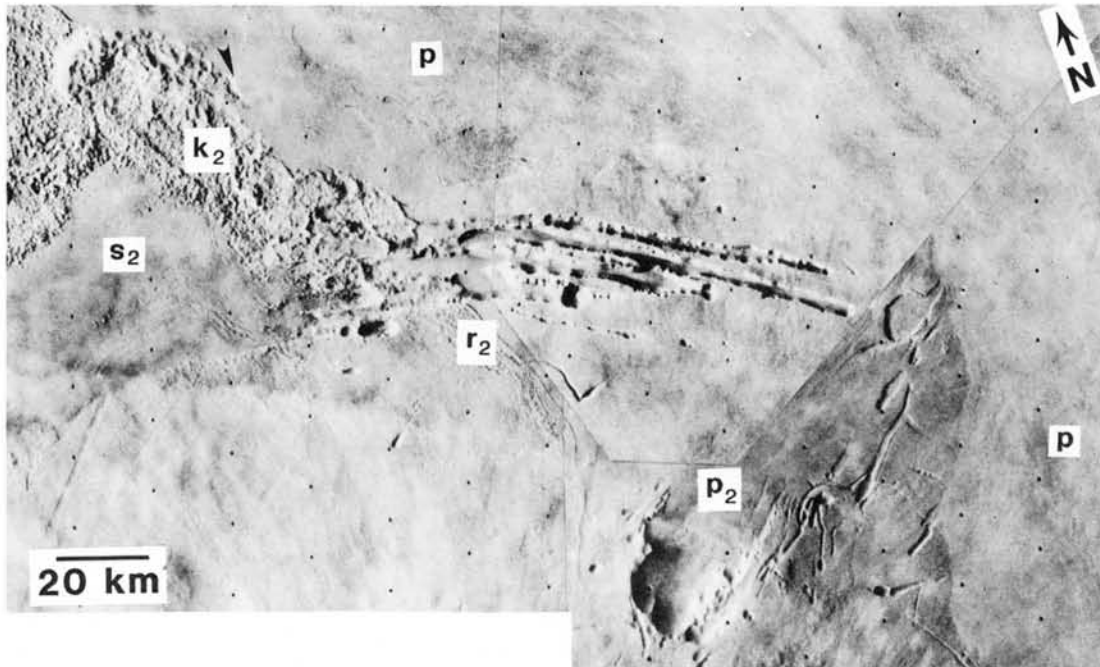


**Fig. 8.** Northern flank vent of Pavonis Mons. Flows that emanate from the northern area are embayed by Tharsis flows (p). The plains lavas also embay a portion of the Pavonis Mons lobe materials (arrow) (mosaic of Viking 49B41,78,80, center at 4.1°N, 111.6°W).

(Thomas *et al.*, 1990). The lower western flank of Ascræus Mons has an irregular scarp at the 10 km elevation, 20 to 30 km above the basal break in slope (Fig. 10). The scarp is similar in overall appearance to the scarp on the west flank of Arsia Mons. Near the northern base of the scarp, a subtle sinuous channel runs from the base of the scarp over smooth shield materials ( $sb_3$ ), interpreted to be fluid lavas that re-surfaced the lower shield (unit  $sb_3$ ) and may have undermined material along the scarp base.

**Flank vents.** The southern and northeastern flanks of Ascræus Mons are intensely channeled by linear and sinuous troughs and grooves, which coalesce into large entrants. Plains emanate from the flank vents ( $p_3$ ) but the last flows, evidenced by subtle linear features interpreted to be flow margins, cross-cut grabens, and other older features. The  $p_3$  flows went primarily north and south, leaving portions of the eastern and western flanks embayed by plains lacking an obvious source (p). The flank vents on Ascræus Mons are smaller and extend a shorter distance into the flanks than the flank vents on the other Tharsis Montes. The numerous troughs and grooves on the flanks may represent the early stages of vent growth as lavas emanated from many closely spaced sources. Prolonged effusion and flank erosion by back-wasting would be required to produce the large Arsia Mons flank vents in this manner.

**Summit.** A nested complex of calderas is present at the summit of Ascræus Mons. Cross-cutting relationships between the caldera floor segments ( $cf_3$ ) indicate that from six (Mouginis-Mark, 1981) to as many as eight (Zimbelman, 1984, p. 75) distinct collapse/flooding events occurred. The central caldera has the largest and only complete floor, indicating it is the last flooding event, and took place in the

deepest caldera (Mouginis-Mark, 1981). The upper portion of the caldera wall is fluted (Fig. 11), similar to the morphology along some upper portions of walls of Valles Marineris (Lucchitta, 1978). The fluted caldera walls have the highest thermal inertia values ( $4 \times 10^{-3} \text{ cal cm}^{-2} \text{ sec}^{-1/2} \text{ K}^{-1}$ ) obtained on the Tharsis volcanos, indicative of semicompetent materials but still an order of magnitude lower than values representative of solid rock (Zimbelman, 1984, p. 145). The lower two-thirds of the caldera wall is relatively featureless at 22 m/pixel resolution, except for faint striations parallel to the slope (Fig. 11). Shadow measurements of the southern caldera wall indicate vertical relief of 2.9 km from the rim to the central caldera floor, which constrains the southern wall to have an average slope  $>26^\circ$  (Zimbelman, 1984, p. 72). The average slope and morphology both suggest that the wall is composed of a talus slope that has accumulated beneath more competent rocks that form the caldera rim, and yet the thermal inertia measurements indicate that the entire caldera area probably has at least several centimeters of fine dust covering virtually the entire visible surface (Zimbelman, 1984, pp. 147-148).

**Lobe-shaped feature.** Ascræus Mons has the smallest of the three lobe-shaped features in the Tharsis region (Fig. 12). The distal portion of the lobe is at an elevation of 5.5 to 7 km, 90 km from the base of the shield along a N85°W trend, with fewer interior deposits than the other lobes (Fig. 2c). Most importantly, a smooth unit is *not* present at Ascræus Mons. Ridged terrain ( $r_3$ ) is present on the distal margin, enclosing knobby terrain ( $k_3$ ) and isolated mountainous areas ( $m_3$ ). Lobate flows ( $l_3$ ), displaying segments of leveed channels, embay the other lobe terrains. The lobate flows may have come from troughs parallel to the shield base, but other plains-

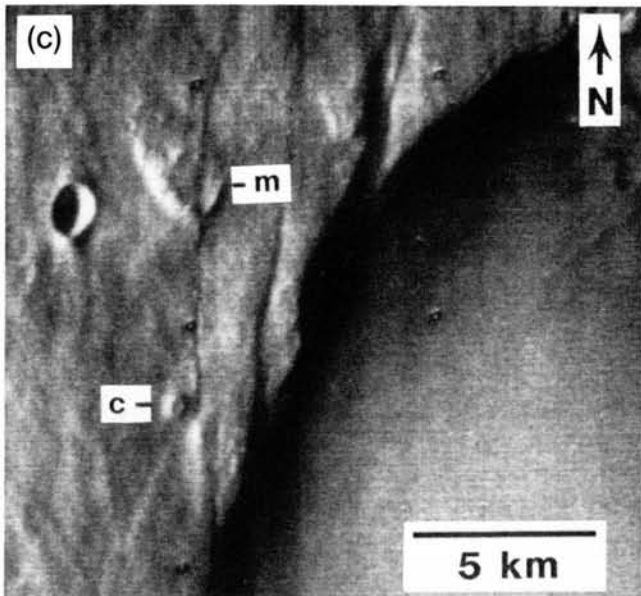
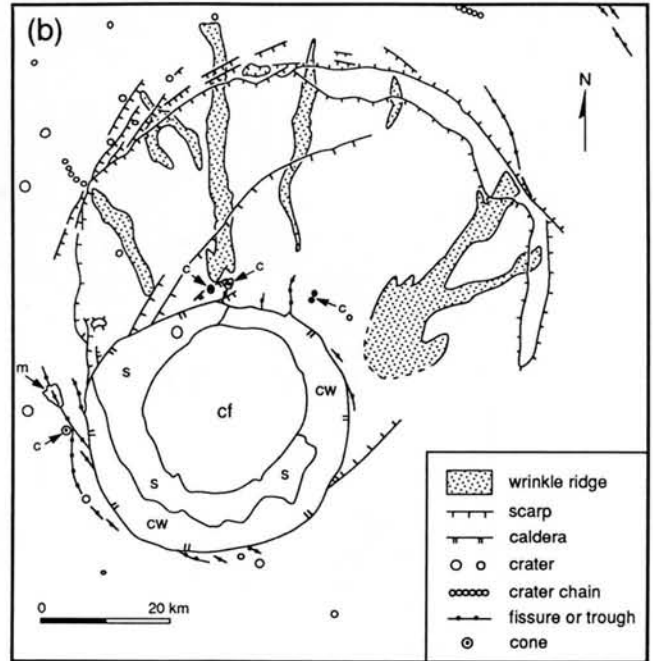
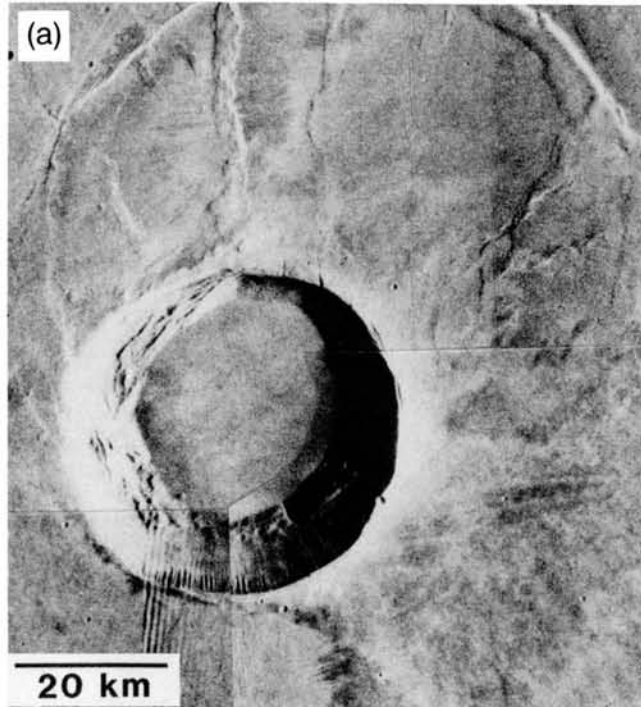


**Fig. 9.** Summit region of Pavonis Mons, centered at 0.9°N, 112.7°W. (a) Photomosaic of Viking images 210A33-36. (b) Sketch map with units cf (caldera floor), s (slumped materials from wall), cw (caldera wall), and m (possible volcanic extrusion that postdates caldera tectonics). Arrows (c) indicate five small cones interpreted to be possible cinder cones. (c) Oblique view of volcanic features near rim of Pavonis Mons caldera. Irregular mound (m) is interpreted to be a volcanic extrusion and cone (c) is interpreted to be a cinder cone, with a basal diameter of 1 km, a height of 70 m, and a summit crater about 450 m in diameter, as originally proposed by Wood (1979) (part of Mariner 9 DAS 55663953, centered at 0.8°N, 113.2°W).

forming lavas (p) truncate the upslope end of the I<sub>3</sub> flows. The Asraeus Mons lobe units occur at elevations below 10 km, adjacent to the western basal scarp. Arcuate scarps outline a segment of the lobe that has dropped *below* all the surrounding terrains (Fig. 2c). The bounding faults to the downdropped block are parallel to the distal margin of the lobe, so the faulting may have been associated with lobe emplacement.

**DISCUSSION**

**General Comparisons**

The observations described above indicate that the geologic development of the three volcanos was similar, yet with some

unique differences not described in previous studies. For example, Pavonis Mons alone appears to have a shield surface that postdates the formation of most grabens and troughs (unit sc<sub>2</sub>). All three Tharsis Montes show evidence of postcaldera summit volcanism, but at Arsia and Asraeus Montes this activity was primarily confined to the calderas while at Pavonis Mons limited strombolian eruptions occurred near the calderas. All three volcanos have coalescing vents on their southern and northeastern flanks, but Pavonis Mons also has small lava deltas on its eastern flank that head at rilles. All three shields have a lobe-shaped feature to the west-northwest, each of which contains similar morphologic units in similar stratigraphic arrangement, but Asraeus Mons lacks the superposed smooth unit (s) present on the other lobes. These subtle differences imply that, while the Tharsis Montes had similar overall histories, each volcano also has a unique variation on the theme.

Numerous individual lava flows can be distinguished in high-resolution Viking images of Asraeus Mons (*Mouginis-Mark*, 1981; *Zimbelman*, 1984, p. 68). Flow dimensions provide calculated yield strengths and viscosities (for Bingham materials) consistent with basaltic or basaltic andesite lavas (*Zimbelman*, 1985). The calculated values are consistent with

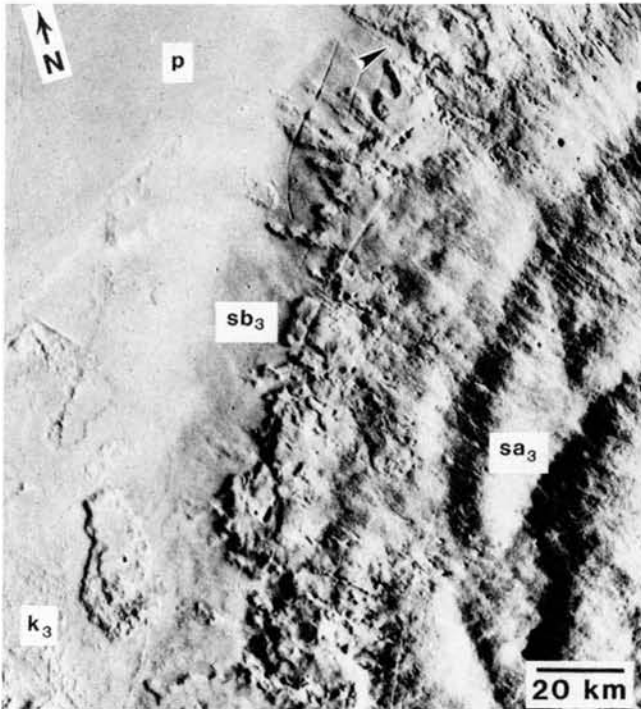


**Fig. 10.** West flank of Ascræus Mons. The upper portion of the flank is terraced and undulatory, while downslope of an irregular scarp the shield surface is relatively smooth and on a uniform level. At the top center, the smooth lower shield unit is crossed by a subtle sinuous channel (arrow) that emanates from the base of the irregular scarp and ends at a small embayment in the shield base. Fluid lavas were likely involved in the resurfacing of the lower shield unit. Rough terrain to the west of the shield ( $k_3$ ) is part of the Ascræus Mons lobe (Viking 892A09, centered at  $12.4^\circ\text{N}$ ,  $107.1^\circ\text{W}$ ).

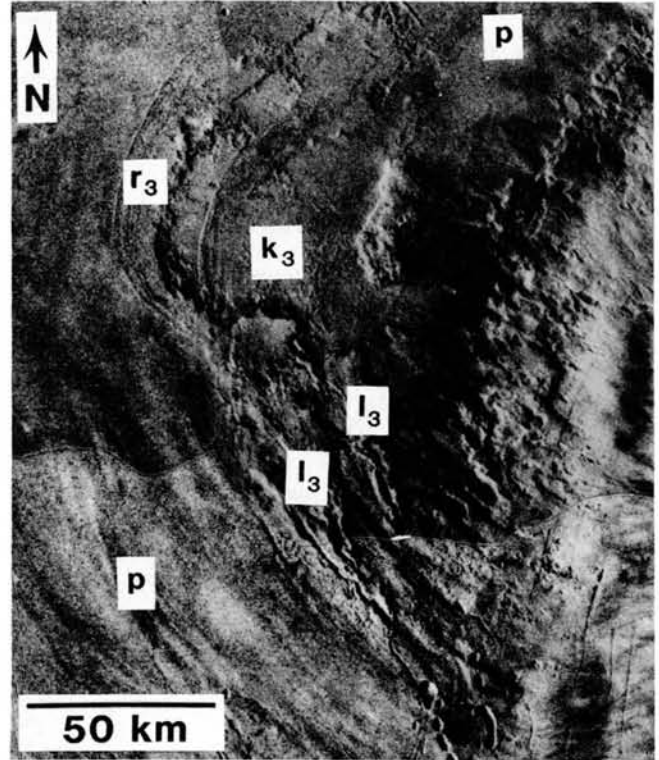


**Fig. 12.** Lobe-shaped feature west of Ascræus Mons. Distal margin is made up of ridged terrain, similar to other Tharsis lobes, with interior knobby terrain. Lobate terrain is embayed on the ridged and knobby units, with leveled channels that extend upslope to troughs near the base of the shield. There is no unit present comparable to the smooth terrain in the other Tharsis lobes (mosaic of Viking 210A10-12, center at  $11.1^\circ\text{N}$ ,  $108.2^\circ\text{W}$ ).

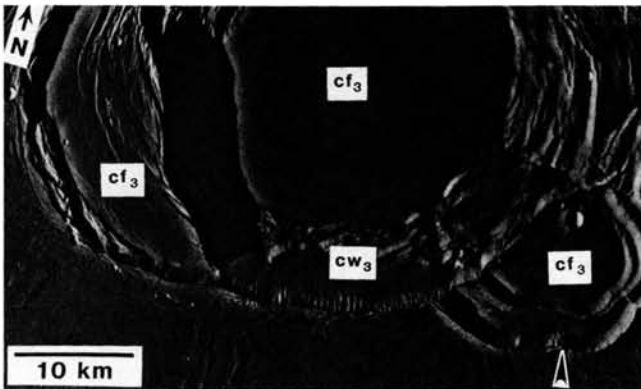


**Fig. 11.** Southern caldera wall of Ascræus Mons. Upper portion of the wall is fluted, indicating the presence of relatively competent materials at the rim. Foot of wall has hummocky deposits that slumped into the caldera. Intermediate wall material is probably a talus slope accumulated beneath the eroded rim. Shadow measurements indicate this wall segment has 2.9 km of vertical relief. Note the truncated, nested calderas at right and a possible dike (arrow) that stands in relief across the uppermost floor segment (digital mosaic of Viking 401B18,20,22, center at  $10.8^\circ\text{N}$ ,  $104.4^\circ\text{W}$ ).

rheologic properties inferred for flows on Arsia Mons (Moore *et al.*, 1978) and Olympus Mons (Hulme, 1976), but are an order of magnitude higher than values obtained for basalt flows on Hawaii (Fink and Zimbelman, 1986, 1990).

#### Modification of Shield Flanks

Irregular scarps along the western margin of Ascræus and Arsia Montes appear to be the result of mass wasting to a level about 300 m below the shield surface. Perhaps the lower portions of the eastern flanks were similarly eroded and have subsequently been covered by plains. However, the elevations of the base of the western flanks are consistently 2 to 3 km lower than the eastern shield bases (USGS, 1989). The lower elevations to the west may have been sufficient to allow magma to rise near the surface and initiate the degradation of the western flanks. While Pavonis Mons lacks a prominent basal scarp, the western flanks of the volcano are degraded relative to adjacent flank surfaces, possibly due to very fluid lava flows.

Carr *et al.* (1977) proposed that the degraded flanks of Arsia Mons represented the detachment surface of a giant landslide that produced the large lobe-shaped deposit northwest of the



volcano. However, the relief along the western scarp indicates that only a limited volume of shield material could have been removed by the hypothesized landslide. The "missing" volume below the scarp is at least an order of magnitude less than the apparent volume of the lobe deposits.

The flank vents on the southwestern and northeastern flanks consist of coalescing channels with blunt headward (upslope) terminations. It seems likely that effusion of fluid lavas transported within the volcanos may be the simplest explanation for not only the flank vents but also the headwall undermining on the lower western flanks. In such a scenario, the flank vents developed where fluid lavas reached the surface close to the trend defined by the overall alignment of the three volcanos, while the western flanks may have experienced sporadic effusion that produced a western basal scarp on two volcanos.

Both the western basal scarps and the flank vent channels appear to represent erosion and/or filling to a common depth. A uniform depth of erosion could be due to a level of more competent materials, such as dense (nonvesicular) basalt, but terrestrial shield volcanos tend to be built of numerous superposed lava flows without obvious volcanowide competent layers (Macdonald, 1972, pp. 272-275). Alternatively, the uniform depth could be the result of fluid lava resurfacing channel floors by consistent internal feeder dike geometries.

### Origin of Lobe-shaped Features

The lobe-shaped features west-northwest of all three Tharsis Montes share common morphologic and relative stratigraphic characteristics, which suggests that they all could have common origins. Two primary origins have been proposed for the lobes: gravity-driven landslides (Carr et al., 1977; Scott and Tanaka, 1986) and ice/debris glaciers (Williams, 1978; Lucchitta, 1981). Carr et al. (1977) dismissed a possible pyroclastic origin, citing the apparent lack of related pyroclastic landforms on the nearby shields, but here we will reexamine this possibility in light of the units present within the lobes. A successful hypothesis for the origin of the lobes must address both the complex arrangements of the associated landforms and the restriction of lobe formation to the western slopes of the volcanos. Considerations of the various landforms visible on the Tharsis lobes lead to problems for both the landslide and glacial origins.

The glacial origin is difficult to reconcile with the observation that the lobes do not resemble the layered and pitted terrains found in and near the martian polar caps, where known ice deposits exist (Sharp, 1973b). All three lobes occur within 15° latitude of the equator, and at elevations between 6 and 10 km, where the present atmospheric water vapor content is low and may prohibit ice accumulation at or near the surface (Figs. 13 and 14 of Farmer et al., 1977).

A landslide interpretation must account for the great size and length of the Tharsis lobes, as well as the lack of obvious source areas of sufficient volume on the adjacent volcanic shields. Two of the largest documented terrestrial subaerial landslides, the Saidmarreh slide in Iran (Harrison and Falcon, 1938) and an ancient avalanche in the Mt. Shasta region of California (Crandell et al., 1984), extend 20 and 40 km, respectively, from their sources. Isolated landslides from steep

scarps within Valles Marineris and around Olympus Mons attain runout lengths of up to 100 km (Sharp, 1973a; Carr et al., 1977; Lucchitta, 1978, 1979), still well short of the 350 and 250 km runout lengths proposed for the Arsia and Pavonis lobes. The slide origin proposed for the Olympus Mons aureole deposits (Tanaka, 1985; Lopes et al., 1982) make these materials the only proposed martian landslide features comparable in scale to the Tharsis lobes. However, the Olympus Mons aureole is morphologically very distinct from the Tharsis lobes (Scott and Tanaka, 1986) and the origin of the aureole deposits remains controversial.

Most of the subaerial terrestrial landslides associated with volcanos occur on slopes >20° (Siebert, 1984). The Tharsis Montes have slopes generally <5°, particularly along their basal flanks, and the adjacent western plains have slopes of 0.5° to at most 2° (USGS, 1989). The great size of the Tharsis lobes is comparable to some terrestrial submarine slides, such as those off the Hawaiian islands (Moore, 1964; Lipman et al., 1988). The submarine landslides originate on shallow slopes more comparable to the slopes around the Tharsis lobes, but the submarine slides have distinctive detachment scarps and other slope failure features that are lacking upslope from the lobe deposits.

A gravity-driven catastrophic slide, perhaps involving pore fluids to reduce friction (e.g., as advocated for the Olympus Mons aureole; Lopes et al., 1982; Francis and Wadge, 1983; Tanaka, 1985), might provide a viable mechanism for the underlying lobe units (r and k), but the lobate flows (l) and smooth (s) terrains must involve additional processes. The lobate flows emanate from troughs in the lower flanks of the volcanos and are superposed on adjacent units, implying that effusive activity postdated the emplacement of the lobes.

We propose that pyroclastic (probably basaltic rather than silicic) activity is an additional volcanic component to the lobe story. Lineations and lobate margins in portions of the smooth unit could be the result of emplacement as a pyroclastic deposit that could have emanated from large grabens within the lobes but off the shield flanks. Pyroclastic activity postdating lobe emplacement possibly was triggered by release of lithostatic load resulting from a slide event. The lack of a smooth unit at Ascræus Mons might result from either insufficient lobe size to unroof a magma chamber or the lack of any near-surface magma west of the volcano. This hypothesis requires further investigation, especially with the improved resolution data from upcoming missions to Mars.

### Synthesis: Geologic Development of the Tharsis Montes

The general development of the Tharsis Montes involved at least seven stages: (1) activity that preceded shield growth, (2) shield construction, (3) caldera formation, (4) flank embayment formation and associated lava emplacement, (5) shield erosion, (6) formation of the large lobe features, and (7) effusive (and pyroclastic?) volcanism following lobe emplacement.

Early work (Carr, 1974; Plescia and Saunders, 1982) indicated that the Tharsis volcanos were preceded by intense fracturing of the martian crust. The shields coalesced from lavas erupted from the fissures along the crest of the Tharsis



rise (Scott and Tanaka, 1981). Calderas formed at the summits of all three volcanoes. All three volcanoes were modified by volcanic eruption from flank vents along the N40°E trend. The western flanks of the shields were modified by mass-wasting and resurfacing by fluid lavas. The lobe-shaped features to the west of each shield are superposed upon all but the youngest of the plains flows. Lobe emplacement was followed by lobate lava flows within all three lobes and deposition of the smooth (pyroclastic?) unit in the lobes at Arsia and Pavonis Montes.

**Acknowledgments.** The authors wish to thank S. Rowland, L. Crumpler, and D. Crown for thorough reviews of the original manuscript, as well as helpful input from M. Robinson. K.S.E. thanks J. W. Branstrator, J. M. Moore, and R. A. Craddock for comments pertaining to the Pavonis Mons study, and P. R. Christensen for advice and support. S. Selkirk provided valuable drafting assistance and D. Ball provided much assistance with the photographs. J.R.Z. received support for this work from NASA grant NAGW-1390 as part of the Mars Geologic Mapping program within the Planetary Geology and Geophysics Program. Portions of this work were carried out while J.R.Z. was a Visiting Scientist at the Lunar and Planetary Institute in Houston, Texas. The Lunar and Planetary Institute is operated by the Universities Space Research Association under grant no. NASW-4574 with the National Aeronautics and Space Administration. This is LPI Contribution 774.

## REFERENCES

- Blasius K. R. (1976) The record of impact cratering on the great volcanic shields of the Tharsis region of Mars. *Icarus*, 29, 343-361.
- Carr M. H. (1973) Volcanism on Mars. *J. Geophys. Res.*, 78, 4049-4062.
- Carr M. H. (1974) Tectonics and volcanism of the Tharsis region of Mars. *J. Geophys. Res.*, 79, 3943-3949.
- Carr M. H., Greeley R., Blasius K. R., Guest J. E., and Murray J. B. (1977) Some martian volcanic features as viewed from Viking Orbiters. *J. Geophys. Res.*, 82, 3985-4015.
- Crandell D. R., Miller C. D., Glicken H. X., Christiansen R. L., and Newhall C. G. (1984) Catastrophic debris and avalanche from ancestral Mount Shasta Volcano, California. *Geology*, 12, 143-146.
- Crumpler L. S. and Aubele J. C. (1978) Structural evolution of Arsia Mons, Pavonis Mons, and Asraeus Mons: Tharsis region of Mars. *Icarus*, 34, 496-511.
- Farmer C. B., Davies D. W., Holland A. L., Laporte D. D., and Doms P. E. (1977) Mars: Water vapor observations from the Viking Orbiters. *J. Geophys. Res.*, 82, 4225-4248.
- Fink J. H. and Zimbelman J. R. (1986) Rheology of the 1983 Royal Gardens basalt flows, Kilauea volcano, Hawaii. *Bull. Volcanol.*, 48, 87-96.
- Fink J. H. and Zimbelman J. (1990) Longitudinal variations in rheological properties of lavas: Puu Oo basalt flows, Kilauea volcano, Hawaii. In *Lava Flows and Domes, IAVCEI Proceedings in Volcanology 2* (J. H. Fink, ed.), pp. 157-173. Springer-Verlag, New York.
- Francis P. W. and Wadge G. (1983) The Olympus Mons aureole: Formation by gravitational spreading. *J. Geophys. Res.*, 88, 8333-8344.
- Greeley R. (1971) Observations of actively forming lava tubes and associated structures, Hawaii. *Mod. Geol.*, 2, 207-223.
- Greeley R. and Gault D. E. (1971) Endogenic craters interpreted from crater counts on the inner wall of Copernicus. *Science*, 171, 477-479.
- Greeley R. and Gault D. E. (1979) Endogenic craters on basaltic lava flows: Size frequency distributions. *Proc. Lunar Planet. Sci. Conf. 10th*, pp. 2919-2933.
- Harrison J. V. and Falcon N. L. (1938) An ancient landslide at Saidmarreh in southwestern Iran. *J. Geology*, 46, 296-309.
- Hartmann W. K. (1973) Martian cratering: IV. Mariner 9 initial analysis of cratering chronology. *J. Geophys. Res.*, 79, 3917-3931.
- Hulme G. (1976) The determination of the rheological properties and effusion rate of an Olympus Mons lava. *Icarus*, 27, 207-213.
- Lipman P. W., Normark W. R., Moore J. G., Wilson J. B., and Gutmacher C. E. (1988) The giant submarine Alika debris slide, Mauna Loa, Hawaii. *J. Geophys. Res.*, 93, 4279-4299.
- Lopes R., Guest J. E., Hiller K., and Neukum G. (1982) Further evidence for a mass movement origin of the Olympus Mons aureole. *J. Geophys. Res.*, 87, 9917-9928.
- Lucchitta B. K. (1978) A large landslide on Mars. *Bull. Geol. Soc. Am.*, 89, 1601-1609.
- Lucchitta B. K. (1979) Landslides in Valles Marineris, Mars. *J. Geophys. Res.*, 84, 8097-8113.
- Lucchitta B. K. (1981) Mars and Earth: Comparison of cold climate features. *Icarus*, 45, 264-303.
- Macdonald G. A. (1972) *Volcanoes*. Prentice-Hall, Englewood Cliffs, New Jersey. 510 pp.
- McCaughey J. E., Carr M. H., Cutts J. A., Hartmann W. K., Masursky H., Milton D. J., Sharp R. P., and Wilhelms D. E. (1972) Preliminary Mariner 9 report on the geology of Mars. *Icarus*, 17, 289-327.
- Moore J. G. (1964) Giant submarine landslides on the Hawaiian Ridge. In *Geological Survey Research 1964, Chapter D*, pp. D95-D98. U.S. Geol. Surv. Prof. Paper 501-D.
- Moore H. J., Arthur D. W. G., and Schaber G. G. (1978) Yield strengths of flows on the Earth, Mars, and Moon. *Proc. Lunar Planet. Sci. Conf. 9th*, pp. 3351-3378.
- Mouginis-Mark P. J. (1981) Late-stage summit activity of martian shield volcanoes. *Proc. Lunar Planet. Sci. 12B*, pp. 1431-1447.
- Neukum G. and Hiller K. (1981) Martian ages. *J. Geophys. Res.*, 86, 3097-3121.
- Plescia J. B. and Saunders R. S. (1979) The chronology of the martian volcanoes. *Proc. Lunar Planet. Sci. Conf. 10th*, pp. 2841-2859.
- Plescia J. B. and Saunders R. S. (1982) Tectonic history of the Tharsis Region, Mars. *J. Geophys. Res.*, 87, 9775-9791.
- Scott D. H. and Carr M. H. (1978) Geologic map of Mars. *U.S. Geol. Surv. Misc. Inv. Series Map I-1083*, scale 1:25,000,000.
- Scott D. H. and Tanaka K. L. (1981) Paleogeographic restoration of buried surfaces in the Tharsis Montes. *Icarus*, 45, 304-319.
- Scott D. H. and Tanaka K. L. (1986) Geologic map of the western equatorial region of Mars. *U.S. Geol. Surv. Misc. Inv. Series Map I-18024*, scale 1:15,000,000.
- Sharp R. P. (1973a) Mass movements on Mars. In *Geology, Seismicity, and Environmental Impact* (D. E. Moran et al., eds.), pp. 115-122. Association of Engineering Geologists, University Publishers, Los Angeles, California.
- Sharp R. P. (1973b) South polar pits and etched terrain. *J. Geophys. Res.*, 78, 4222-4230.
- Siebert L. (1984) Large volcanic debris avalanches: Characteristics of source areas, deposits, and associated eruptions. *J. Volcanol. Geotherm. Res.*, 22, 163-197.
- Tanaka K. L. (1985) Ice-lubricated gravity spreading of the Olympus Mons aureole deposits. *Icarus*, 62, 191-206.
- Thomas P. J., Squyres S. W., and Carr M. H. (1990) Flank tectonics of martian volcanoes. *J. Geophys. Res.*, 95, 14345-14355.
- USGS (U.S. Geological Survey) (1989) Topographic maps of the western, eastern equatorial and polar regions of Mars. *U.S. Geol. Surv. Misc. Inv. Series Map I-2030*, scale 1:15,000,000.

- Whitford-Stark J. L. (1982) Tharsis volcanoes: Separation distances, relative ages, sizes, morphologies, and depths of burial. *J. Geophys. Res.*, 87, 9829-9838.
- Williams H. and McBirney M. A. (1979) *Volcanology*. Freeman, Cooper & Co., San Francisco. 397 pp.
- Williams R. S. (1978) Geomorphic processes in Iceland and Mars: A comparative appraisal from orbital images (abstract). *Geol. Soc. Am. Abstr. with Program*, 10, 517.
- Wood C. A. (1979) Monogenetic volcanoes of the terrestrial planets. *Proc Lunar Planet. Sci. Conf. 10th*, pp. 2815-2840.
- Zimbelman J. R. (1984) Geologic interpretation of remote sensing data for the martian volcano Ascraeus Mons. Ph.D. dissertation, Arizona State University, Tempe. In *Advances in Planetary Geology*, pp. 271-572. NASA TM-88784.
- Zimbelman J. R. (1985) Estimates of rheologic properties for flows on the martian volcano Ascraeus Mons. *Proc. Lunar Planet. Sci. Conf. 16th*, in *J. Geophys. Res.*, 90, D157-D162.
- Zimbelman J. R., Solomon S. C., and Sharpton V. L. (1991) The evolution of volcanism, tectonics, and volatiles on Mars: An overview of recent progress. *Proc. Lunar Planet. Sci., Vol. 21*, pp. 613-626.